Light Metals 2014
Edited by: John Grandfield
TMS (The Minerals, Metals & Materials Society), 2014

Modelling HF Generation: The Role of Ambient Humidity

Youjian Yang[1], Margaret Hyland[2], Chris Seal[2], Zhaowen Wang[1]
[1]School of Materials and Metallurgy, Northeastern University, Mail Box 117, Shenyang, China
[2]Light Metals Research Centre, University of Auckland, Private Bag 92019, Auckland, New Zealand

Keywords: Hydrogen fluoride, ambient humidity, dissolved hydroxide, ambient moisture

Abstract

HF generation in aluminium reduction cells is known to occur by the reaction between fluorides (in a variety of forms) and a source of water or hydrogen. Studies on the generation of HF indicate that the major sources of moisture for hydrogen fluoride generation appear to be alumina, in the form of structural hydroxides (LOI 300-1000) and adsorbed moisture (LOI 25-300), and the ambient humidity. Several models have been developed to estimate the amount of hydrogen fluoride generated but these do not consider the individual sources of fluoride generation and cannot be easily used to assess the impact of changes in relative humidity. This paper presents a new model, still under development, which simulates the hydrolysis of pot gas from an open feeder hole. Initial results suggest that, in an open feeder hole, the high background concentration of hydrogen fluoride (3000–5000 ppm) presents, inhibiting the hydrolysis of pot gas, and thus the ambient humidity has relatively limited influence on the total fluoride emission. While the influence of ambient humidity has been the focus of this study, the model developed is intended to provide a framework that can be used to assess the sensitivity of fluoride emissions to other factors.

Introduction

Generally, the moisture or hydrogen for HF formation in aluminium reduction cells is introduced by moisture from alumina, fluoride additives, ambient humidity and anode hydrogen [1, 2]. For different types of anodes, hydrogen content varies from 0.003% to 0.1% and hydrolysis only occurs along with electrolysis with an average efficiency of nearly 25% [3]. Moisture in alumina exists in two forms: one is the absorbed water (LOI 25-300 or MOI), the other is residual hydroxyl from gibbsite (LOI 300-1000 or structural water). Part of alumina structural water dissolves with alumina into molten bath, enjoying a long residence time. Due to continuous feeding and stable consumption in electrochemical hydrolysis with bath, this hydrogen source could produce a HF background in the original pot gas [4]. In addition, most of the alumina adsorbed moisture flashes off before hitting the high temperature molten bath [5, 6]. The flashed-off alumina moisture combines with ambient humidity and reacts with bath vapour and entrained bath at high temperature feeder holes, tap holes or cracks in the crust [7, 8]. A summary of hydrogen sources and hydrolysis pathways in the reduction cell is shown in Fig.1. Generally, alumina structural water and anode hydrogen contribute to the electrochemical hydrolysis of liquid bath, while alumina MOI, ambient air moisture and unreacted alumina structural water/anode hydrogen contribute to the thermal hydrolysis of pot gas.

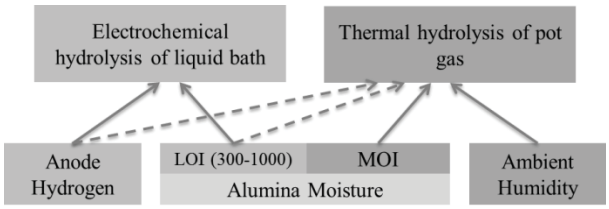

Fig.1 Different sources of hydrogen contribute to different ways for HF formation

For the electrochemical reactions of anode hydrogen and dissolved hydroxide, the main fluoride species is believed to be AlF_3 because the equilibrium coefficient for AlF_3 is over a thousand times higher than other species like Na_3AlF_6 or $Na_5Al_3F_{14}$ under reasonable temperature for aluminium reduction [1, 9, 10]. For the thermal hydrolysis of the fume, sometimes the CO in pot gas causes flaming while discharging from holes, which would promote the local temperature to as high as 1200-1400^oC [11]. In this way, the HF formation from the reactions of Na_3AlF_6 and $Na_5Al_3F_{14}$ species should also be included. Reactions for HF formation are listed as follows.

$$3NaAlF_{4(g)} + 3H_2O_{(g)} \rightarrow 6HF_{(g)} + Al_2O_{3(s)} + Na_3AlF_{6(l/s)} \quad (1)$$

$$2AlF_{3(l)} + 3H_2O_{(g)} \rightarrow 6HF_{(g)} + Al_2O_{3(s)} \quad (2)$$

$$3Na_5Al_3F_{14(g/l)} + 6H_2O_{(g)} \rightarrow 12HF_{(g)} + 5Na_3AlF_{6(l/s)} + 2Al_2O_{3(s)} \quad (3)$$

$$2Na_3AlF_{6(l)} + 3H_2O_{(g)} \rightarrow 6HF_{(g)} + 6NaF_{(s)} + Al_2O_{3(s)} \quad (4)$$

Haupin built an empirical-mathematical HF emission model in 1993 [1]. Based on thermodynamics and empirical kinetics, his model matches well with a 170kA Alcoa cell [12]. HF from fume hydrolysis was estimated with an empirical formula in which the contribution from ambient humidity and alumina flashed-off moisture was not distinguished. In his model, HF generation from fume hydrolysis could reach up to approximately 30% of total HF emission and 15% of total fluoride emission. One of the bath chemistries in the model introduced in this paper was chosen to be the same as Haupin's model.

Patterson has proved the theory that dissolved hydroxide is the major contributor to HF generation during electrolysis, which also matches well with the measurement of HF concentration in the original pot gas. From his estimate, in different smelters, the HF emission due to ambient humidity varies from 10% to 30% of total HF amount [4].

Osen and Sommerseth did measurements of HF concentration at different positions in 300kA Hydro cell and 170kA Alcoa cell [13, 14]. They have found that there is a HF background when they put the probe in the non-flaming tap hole and flaming feeder hole, both centimetres above the bath. The schematic for HF measurement is show in Fig.2. It is believed that the HF level in

non-flaming holes (Measurement position 1, 3000-5000ppm) represents the HF background in the pot gas.

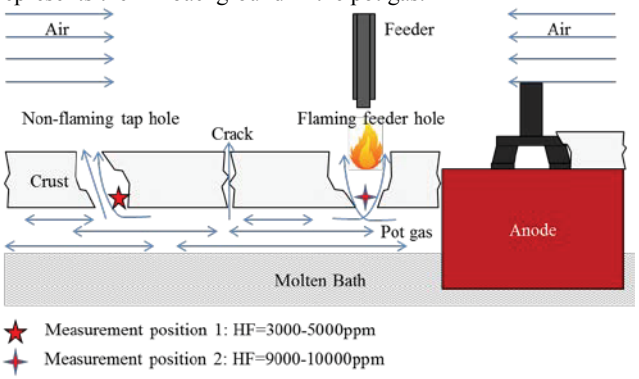

Fig.2 Schematic for HF background measurement [13, 14]

Modelling

A model of HF emission was built using multiple software packages including ANSYS Flotran (Built-in CFD), HSC Chemistry and MATLAB. Temperature gradients in and around a feeder hole were simulated with Ansys 10.0, for with and without flaming scenarios. HSC Chemistry 6.0 was used to calculate the equilibrium composition of fluoride species in the fume with different temperatures, fluoride species and ambient humidity. Matlab R2009a was used to collect simulation results from the software mentioned above and do the final calculation. The flowchart of the modelling is shown in Fig.3.

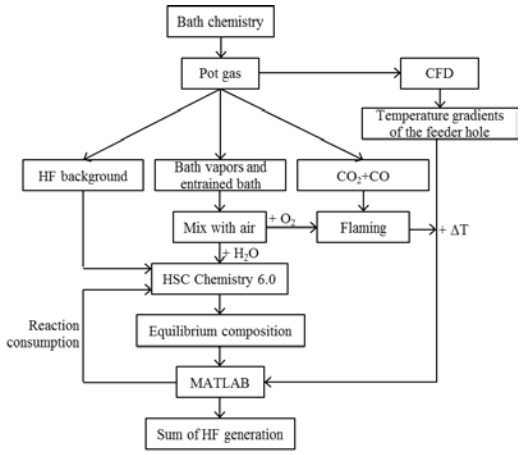

Fig.3 The flowchart for the procedures of the modelling

Three different bath chemistries in a 170kA smelter were tested with the model. The cell parameters and bath chemistry 1 were chosen to be the same as the parts in which Haupin's model displayed the best reproducibility [1]. Bath chemistry 2 and 3 were chosen to represent typical Chinese and western aluminum baths respectively. The parameters of the cell are listed in Table 1.

Table 1 Definition of the parameters of a single cell in this model

Parameter		Value
Current (kA)		170
Voltage (V)		4.2
CE (%)		90
Size of the feeder hole, Ø × h (m)		Ø0.2×0.2
Number of feeder holes		4
Ambient air pressure (bar)		1
Bath Chemistry 1 (From Haupin's Model [1])	Cell Temperature (^oC)	988 (with 15^oC superheat)
	n(NaF)/n(AlF_3)	2.8
	Al_2O_3 (%)	3.0
	MgF_2 (%)	0.15
	CaF_2 (%)	6.5
Bath Chemistry 2 (Typical Chinese Bath)	Cell Temperature (^oC)	936 (with 10^oC superheat)
	n(NaF)/n(AlF_3)	2.4
	Al_2O_3 (%)	3
	LiF (%)	5
	MgF_2 (%)	1
	CaF_2 (%)	5
Bath Chemistry 2 (Typical Western Bath)	Cell Temperature (^oC)	962 (with 10^oC superheat)
	n(NaF)/n(AlF_3)	2.15
	Al_2O_3 (%)	3
	CaF_2 (%)	5

Simulation of the temperature gradients

Fig.4 shows the schematic of the CFD model. High temperature pot gas was injected from the bottom of the feeder hole, with a velocity of approximately 0.31 m/s (varies with cell temperature, calculated from total pot gas volume for per tonne aluminium production). Cool air carrying moisture and oxygen from sides mixed with the pot gas, causing flaming of the CO and hydrolysis of bath vapour and entrained bath. An assumption was made that the air above crust was preheated to a 200^{o}C level by crust/anodes. The original velocity of the air was set as 1.0 m/s which was calculated from the 3400Nm^3/(h·cell) duct suction [15]. The temperature of the hoods was set as 120^{o}C, while the temperature of the injected pot gas and crust bottom were simulated from a solid Ansys model by using an empirical convection coefficient of 10 W/(m^2·K) as shown in Fig.5.

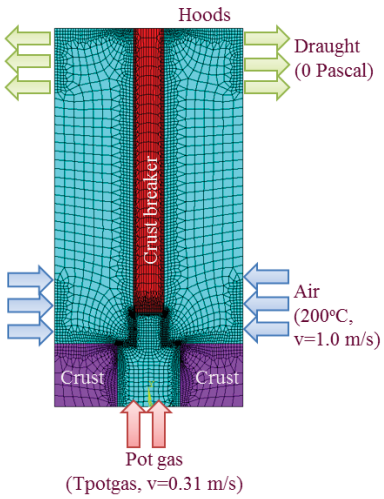

Fig.4 The schematic of the CFD model

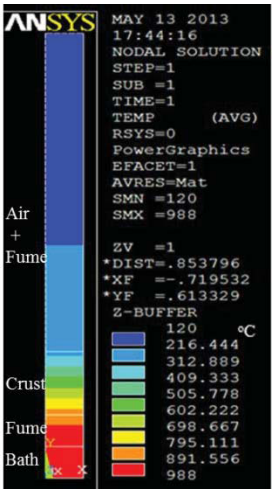

(a) Solid model of a slice of crust with bath chemistry 1

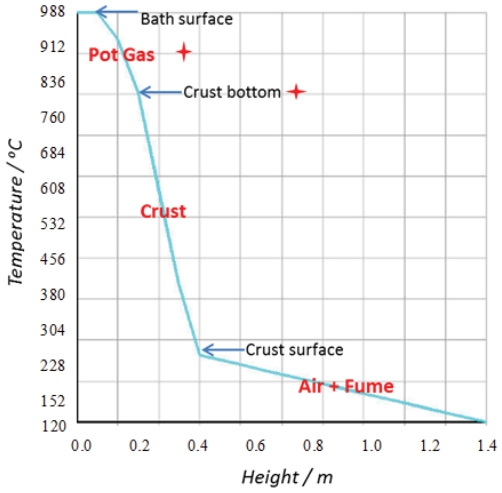

(b) Temperature changes with height for Fig 4 from the bottom to the top

Fig.5 Ansys simulation using an empirical convection coefficient in a solid model with no fluid flow, aiming to obtain the temperature of pot gas and crust bottom for the model shown in Fig.4, where the temperature of the pot gas was set as the average temperature of crust bottom and liquid bath.

Fig. 6 and 7 shows the velocity vectors and temperature gradients for the flaming and non-flaming feeder hole scenarios respectively. With a CE of 90%, the proportion of CO in the pot gas is approximately 20% according to Pearson-Waddington's formula [16]. As nearly 50% of the CO combusts when in contact with air [11], the combustion heat from the flaming would heat the pot gas up by nearly 480°C.

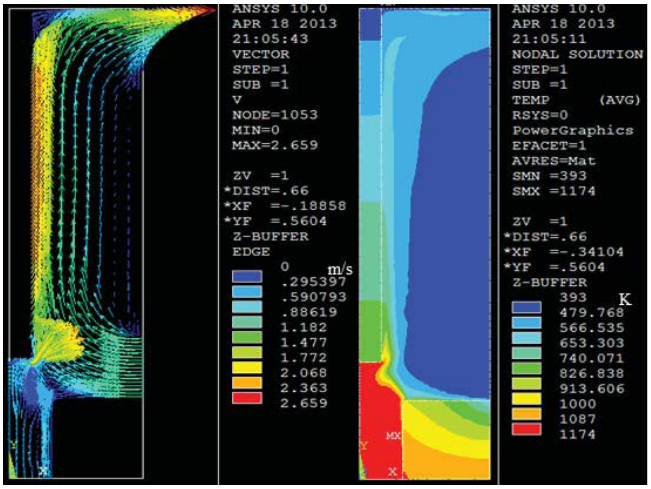

(a) Velocity vectors (b) Temperature gradient

Fig.6 Ansys Flotran simulation of a 1/2 slice non-flaming feeder hole with bath chemistry 1

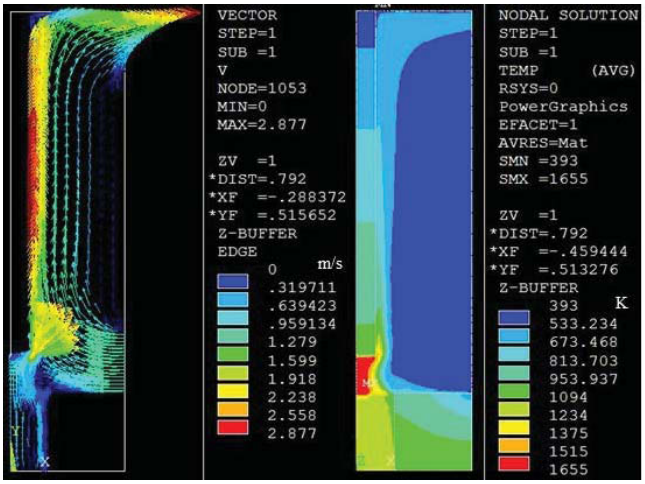

(a) Velocity vectors (b) Temperature gradient

Fig.7 Ansys Flotran simulation of a 1/2 slice flaming feeder hole with bath chemistry 1

From Fig.6a and 7a, the turbulent airflow generally flowed along the surface of the crust breaker. The speed of the draught could reach up to approximately 2.7-2.9 m/s. Air coming from sides mixed with the hot pot gas and cooled the fume and crust down. Fig.6b and 7b shows the corresponding temperature gradients. The area above feeder hole experiences a higher temperature than the crust. The cool air above the crust also cooled the crust down to a reasonable range. In Fig.7b, due to 50% of the CO

combusting and flaming when contacting with air, the local temperature could be as high as 1382°C.

Original fluoride species in the pot gas

Particulate fluoride evolved from aluminum cells results from vaporization of the liquid bath and entrained bath droplets. In this model, an assumption was made that CO_2 and CO escape from the bath carrying an equilibrium partial pressure of bath species. The volatilization of the bath and entrained bath were calculated with Haupin's formula [1, 5, 17]. The original fluoride species entrained in the pot gas for input into the model are listed in Table 2.

Table 2 The particulate fluoride species and HF background of the original pot gas

Classification	Content	Bath Chemistry		
		1	2	3
Volatilization of bath (mol/tonne Al)	$NaAlF_4$	109.67	68.58	161.40
	$(NaAlF_4)_2$	1.38	1.11	4.24
	NaF	4.80	1.90	0.82
Entrained bath (mol/tonne Al)	Na_3AlF_6	66.16	62.39	34.43
	$Na_5Al_3F_{14}$	3.89	7.24	20.18
Total particulate fluoride including bath vapor and entrained bath (kgF/tonne Al)		17.21	14.46	22.22
Background HF level (mol/tonne Al)	HF	203.84 - 339.74 (Based on 3000 - 5000ppm as measured in the tap hole [13])		

The Chinese bath chemistry 2 usually contains more additives such as LiF, MgF_2 and KF than western bath. However, LiF acts to pull the vapor pressure of the bath down greatly [18-22]. Hence, the fluoride emission of the western bath chemistry 3 is much more than that of bath chemistry 2. The total fluoride losses including particulate and gaseous fluoride were 23.67, 20.91 and 28.68 kg F/tonne Al, respectively for bath chemistries 1, 2, 3.

Equilibrium composition from HSC Chemistry

In this part, equilibrium was assumed because fluoride species react fast under high temperatures. Reactions below 680°C were neglected in consideration of low reaction rate of condensed particulate [23]. With given fluoride species, water content, pressure and temperature, HSC Chemistry 6.0 was able to calculate the equilibrium composition using hydrolysis reactions (1) to (4) and any other possible reactions. The HF generation from hydrolysis of the original pot gas with different water content is shown in Fig.8.

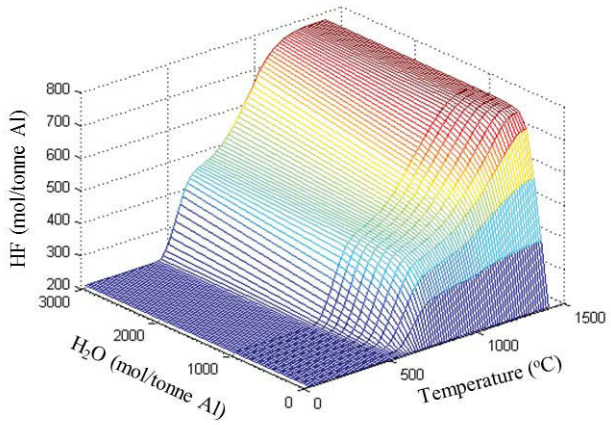

Fig.8 Equilibrium composition of the following hydrolysis of the original pot fume with varied water and temperatures with bath chemistry 1 and HF background of 3000ppm

The fluoride species might reach equilibrium at high temperatures in a very short time, but as the temperatures reduce, the equilibrium would go towards the negative direction. The HF generation was calculated through the average equilibrium of all the mesh grids in the CFD model. In each grid, the proportion of mixing air and pot gas in the fume was determined according to heat balance in which the way of heat transfer was assumed to be only convection.

Molar proportion of air and pot gas at different temperatures is given by the equation:

$$\frac{n_{potgas}}{n_{air}} = \frac{C_{air} \cdot M_{potgas} \cdot (T_{ave} - T_{air})}{C_{potgas} \cdot M_{air} \cdot (T_{potgas} + \Delta T - T_{ave})} \quad (5)$$

Where:

C_{air} = *Specific heat of air, J/(kg·K);*
C_{potgas} = *Specific heat of the pot gas, J/(kg·K);*
M_{air} = *Average molar mass of air, g/mol;*
M_{potgas} = *Average molar mass of the pot gas, g/mol;*
T_{ave} = *Average temperature of the grid, K;*
T_{air} = *Original temperature of the injected air, K;*
T_{potgas} = *Original temperature of the injected pot gas, K;*
ΔT = *Temperature increase caused by CO combusting and flaming, if present, K.*

Results and Discussions

As mentioned above, the HF background would account for 3.87-6.46 kg F/tonne Al gaseous fluoride loss (3000-5000ppm). These initial levels of HF in the pot gas would affect the equilibrium of the hydrolysis reactions (1) to (4), inhibiting the HF formation. The HF generation due to fume hydrolysis with ambient moisture is shown in Fig.9.

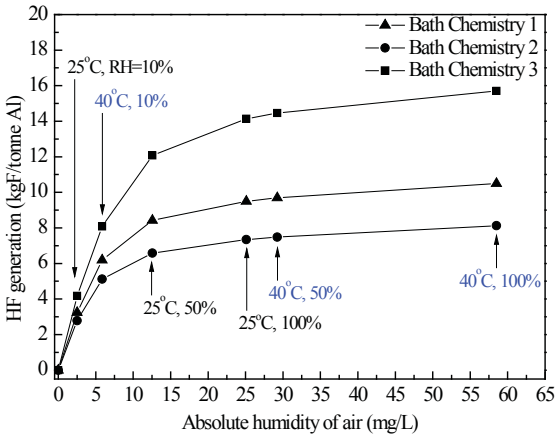

Fig.9 HF generation from fume hydrolysis with ambient moisture, all the pot gas discharging from flaming feeder holes with HF background of 5000ppm, AH refers to absolute humidity, RH refers to relative humidity.

As can be seen from Fig.9, the HF generation at equilibrium increased rapidly with absolute humidity at first and then became flattened. It suggests that the HF generation from ambient humidity is controlled by the equilibrium. With CO combusting and flaming in the feeder holes, the HF generation due to ambient humidity could reach up to nearly 16 kg F/tonne Al with bath chemistry 3 when the temperature in pot room was 40°C, RH=100%, which is the normal condition for aluminium plants located in hot humid places. Under the same ambient humidity, the HF generation was greatly determined by the amount of fluoride species, which varied with different bath chemistries. With 50% of the CO flamed as contacting with air, 60-70% maximum of the particulate fluoride reacted to form HF.

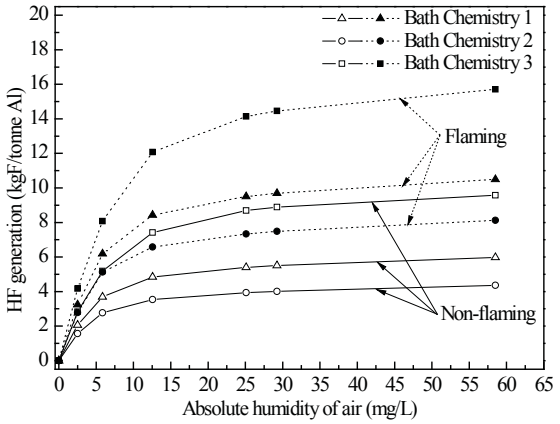

Fig.10 HF generation from fume hydrolysis with ambient moisture, all the pot gas discharging from non-flaming feeder holes with HF background of 5000ppm

If all the pot gas discharges from flaming holes, the average reaction temperature for the fume hydrolysis was approximately 960°C (slightly different with bath chemistry), which was 100-120°C higher than that of non-flaming condition. Therefore the higher equilibrium temperature directly led to a higher proportion of pot gas hydrolysis. From Fig.10, the HF generation from bath chemistry 3 at ambient humidity of 40°C, RH=100% was approximately 10 kg F/tonne Al. The non-flaming condition could be obtained by keeping a good integrity of the crust. In this way, the HF emission from ambient humidity hydrolysis could be cut down by 40-45%. Better cover of the cell could also lower the amount of entrained bath discharged from holes in the crust.

The ambient moisture hydrolysis is also influenced by the initial HF background in the pot gas. Therefore assumed HF background levels were brought in the model to see how much they could affect the hydrolysis reactions. Fig.11 shows the HF generation from ambient moisture with bath chemistry 1 and different HF background levels.

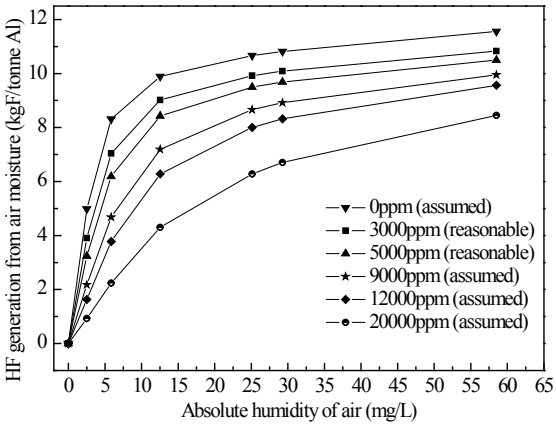

Fig.11 HF generation from fume hydrolysis with ambient moisture under assumed HF background, all the pot gas discharging from flaming feeder holes, bath chemistry 1

As is shown in Fig.11, the higher the HF background, the less HF generated from thermal hydrolysis of ambient humidity. Within the reasonable range of 3000-5000ppm background, HF from ambient humidity hydrolysis did not vary much with a difference less than 0.8kg F/tonne Al. The curves with higher HF background resulted in smaller initial slopes, suggesting greater resistance for reactions (1) to (4) to proceed in the forward direction. Since the non-flaming model indicates good crust condition, a table summarizing HF emissions in varying ambient humidity conditions, with different bath chemistries and for different crust conditions are shown in Table 3.

Table 3 HF emissions due to ambient humidity with typical Chinese and western bath chemistries

Bath chemistry	HF emission due to ambient humidity (kg F/tonne Al)			
	Good crust condition (Non-flaming model)		Poor crust condition (Flaming model)	
	Dry air	Wet air	Dry air	Wet air
1 - Old bath (Haupin)	2-4	5-6	3-7	9-11
2 - Chinese bath	1-3	4-5	3-6	7-9
3 - Western bath	3-6	9-10	4-9	14-16

Conclusion

In this model, HF generation from ambient humidity was estimated when the pot gas flowed through an open feeder hole. It was found that the HF from air moisture is greatly dependent on the ambient humidity and is controlled by the equilibrium of

hydrolysis reactions. For poor crust condition, the flaming model showed that HF generation could reach up to 9-16 kgF/t Al, contributing to 60-70% of the gaseous fluoride. By keeping a good integrity of the crust to avoid the CO combustion, this part of HF generation could be cut down by nearly 40-50%.

Acknowledgements

This work was supported by the National Basic Research Program of China (No. 2007CB210305), The National Natural Science Foundation of China (Grant No. 51074045), National Key Technology R&D Program (No. 2012BAE08B01) and China Scholarship Council (CSC).

The authors would like to acknowledge the helpful advice from Prof. Barry Welch.

References

1. Haupin, W. and H. Kvande, *Mathematical Model of Fluoride Evolution from Hall‐Héroult Cells.* Essential Readings in Light Metals: Aluminum Reduction Technology, Volume 2, 1993: p. 903-909.
2. Haupin, W.E., *Mathematical Model of Fluoride Evolution from Hall‐Héroult Cells.* Light Metals, 1984: p. 11.
3. Patterson, E., M. Hyland, V. Kielland, and B. Welch, *Understanding the effects of the hydrogen content of anodes on hydrogen fluoride emissions from aluminium cells.* Light Metals, 2001: p. 365-370.
4. Patterson, E.C., *Hydrogen Fluoride Emissions from Aluminium Electrolysis Cells*. 2002, ResearchSpace@ Auckland, PhD Thesis, The University of Auckland.
5. Grjotheim, K., H. Kvande, K. Motzfeldt, and B. Welch, *The formation and composition of the fluoride emissions from aluminum cells.* Canadian Metallurgical Quarterly, 1972. **11**(4): p. 585-599.
6. Henry, J.L., *A Study of Factors Affecting Fluoride Emission from 10,000 Ampere Experimental Aluminum Reduction Cells.* Essential Readings in Light Metals: Aluminum Reduction Technology, Volume 2, 1963: p. 855-864.
7. Hyland, M., B. Welch, and J. Metson, *Changing knowledge and practices towards minimising fluoride and sulphur emissions from aluminium reduction cells.* Light Metals, 2000: p. 333-338.
8. Slaugenhaupt, M.L., J.N. Bruggeman, G.P. Tarcy, and N.R. Dando. *Effect of open holes in the crust on gaseous fluoride evolution from pots*. Light Metals, 2003: p.199-204.
9. Grjotheim, K. and B.J. Welch, *Aluminium smelter technology: a pure and applied approach*. 1980: Aluminium-Verlag Dusseldorf.
10. Haupin, W.E. and W.B. Frank, *Electrometallurgy of aluminum*, in *Comprehensive Treatise of Electrochemistry*. 1981, Springer. p. 301-325.
11. Dorreen, M.M.R., *Cell performance and anodic processes in aluminium smelting studied by product gas analysis*. 2000, ResearchSpace@ Auckland, PhD Thesis, The University of Auckland.
12. Wahnsiedler, W., R. Danchik, D. Backenstose, W. Haupin, and J. Colpitts, *Factors Affecting Fluoride Evolution from Hall‐Heroult Smelting Cells.* Light Metals, 1978: p. 9.
13. Sommerseth, C., K.S. Osen, T.A. Aarhaug, E. Skybakmoen, A. Solheim, C. Rosenkilde, and A.P. Ratvik, *Correlation between Moisture and HF Formation in the Aluminium Process.* Light Metals 2011: p. 339-344.
14. Osen, K.S., T.A. Aarhaug, A. Solheim, E. Skybakmoen, and C. Sommerseth, *HF measurements inside an aluminium electrolysis cell.* Light Metals, 2011.
15. Abbas, H., *Mechanism of top heat loss from aluminium smelting cells*. 2010, ResearchSpace@ Auckland, PhD Thesis, The University of Auckland.
16. Pearson, T. and J. Waddington, *Electrode reactions in the aluminium reduction cell.* Discussions of the Faraday Society, 1947. **1**: p. 307-320.
17. Less, L. and J. Waddington, *The characterisation of aluminium reduction cell fume.* Essential Readings in Light Metals: Aluminum Reduction Technology, Volume 2, 1971: p. 865-869.
18. Gustavsen, Ø.T. and T. Østvold, *Effect of LiF on the vapour pressure over cryolite containing melts.* Light Metals 2001: p. 357-364.
19. Cassayre, L., P. Palau, P. Chamelot, and L. Massot, *Properties of Low-Temperature Melting Electrolytes for the Aluminum Electrolysis Process: A Review.* Journal of Chemical & Engineering Data, 2010. **55**(11): p. 4549-4560.
20. Jaimes, J.G., *Vaporization of Molten Fluorides*. 1986, Inst. for Uorganisk Kjemi, Norges Tekniske Høgskole, Trondheim, Norway, Avhandling.
21. Jaimes, J.G., *Vaporization of molten fluorides: the systems, sodium fluoride-aluminium fluoride, cryolite-alkali fluoride, and cryolite-alkaline earth fluoride*. 1986, PhD Thesis, Inst. for Uorganisk Kjemi, Norges Tekniske Høgskole
22. Zhou, H.-h., O. Herstad, and T. Ostvold. *Vapour pressure studies of and complex formation in NaF-AlF3 and Na3AlF6-MgF2 melts*. in *Proceedings of the 121st TMS Annual Meeting, March 1, 1992 - March 5, 1992*. 1991. San Diego, CA, USA: Publ by Minerals, Metals & Materials Soc (TMS).
23. Bjorseth, O., O. Herstad and J. L. Holm, *On the physical and thermodynamic stability of solid sodium tetrafluoro-aluminate.* Acta chemica Scandinavica. Series A. Physical and inorganic chemistry, 1986. **40**(9): p. 566-571.